Received: 27 April 2020 | Revised: 25 May 2020 | Accepted: 27 May 2020

DOI: 10.1002/ppap.202000090

PLASMA PROCESSES AND POLYMERS

FULL PAPER

Controlled co-immobilization of biomolecules on quinone-bearing plasma polymer films for multifunctional biomaterial surfaces

Urszula Czuba[1,2] | **Maryline Moreno-Couranjou**[1] | **Delphine Collard**[3] | **Marie-Claire De Pauw-Gillet**[4] | **Robert Quintana**[1] | **Patricia Lassaux**[5] | **Christophe Detrembleur**[2] | **Patrick Choquet**[1]

[1]Department of Materials Research and Technology, Luxembourg Institute of Science and Technology (LIST), Belvaux, Luxembourg

[2]CESAM Research Unit, Department of Chemistry, Center for Education and Research on Macromolecules (CERM), University of Liege, Liège, Belgium

[3]Department of Environmental Research and Innovation, Luxembourg Institute of Science and Technology (LIST), Belvaux, Luxembourg

[4]Department of Mammalian Cell Culture Laboratory–Chemistry, University of Liège, Liège, Belgium

[5]Molecular Biomimetic and Protein Engineering Laboratory (MBPEL), GIGA-R, University of Liège, Liège, Belgium

Correspondence
Maryline Moreno-Couranjou, Department of Materials Research and Technology, Luxembourg Institute of Science and Technology (LIST), L-4422 Belvaux, Luxembourg.
Email: maryline.moreno@list.lu

Funding information
Direction Générale Opérationnelle de l'Economie, de l'Emploi et de la Recherche (DG-06) Belgique, région Wallonie, Grant/Award Number: (METABIO/no. convention 111278 and 1318213); Fonds National de la Recherche Luxembourg, Grant/Award Number: BIOREAFILM (C15/MS/10365992/BIOREAFILM/Moreno), METABIO (FNR INTER/MAT/13/13)

The copyright line was changed on 30 June 2020 after original publication.

Abstract

In this study, an efficient methodology, allowing the controlled co-immobilization of two complementary biomolecules, is reported for the production of multifunctional antibacterial surfaces. To promote long-lasting covalent immobilization, metallic surfaces are first coated with a quinone-bearing poly (methacrylate)-based thin film by combining an atmospheric pressure liquid-assisted plasma polymerization and a controlled sodium periodate-induced catechol oxidation steps. The influence of the oxidation step on the film morphology and chemistry is investigated using an analytical multitool approach involving atomic force microscopy, ultraviolet, infrared, and X-ray photoelectron spectroscopy techniques. Quartz crystal microbalance with dissipation monitoring (QCM-D) analyses allow the rapid determination of the optimal biomolecule immobilization conditions in terms of kinetics of grafting and biomolecule solution concentrations. In vitro functional assays combined with QCM-D analyses demonstrate promising, dual biologically active coated surfaces.

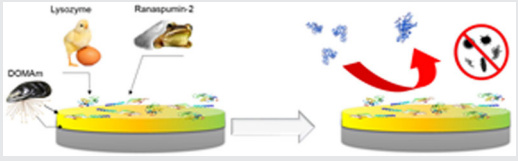

KEYWORDS

antibacterial coatings, biomaterials, dielectric barrier discharges, immobilization of biomolecules, plasma polymerization

1 | INTRODUCTION

Biomaterials play a fundamental role in disease management and the improvement of health care. Among various existing biomaterials, titanium and titanium alloys are the most commonly used metallic materials for implantation in the human body for orthopedic or dental surgeries.[1] Despite their extensive use, titanium alloys are unable to integrate directly with the adjacent bone tissue. Thus, metallic prostheses constantly appear to be encapsulated by a layer of connective tissue. At the same time, the susceptibility of the implant surface to bacterial colonization and biofilm formation remains a major problem, leading to implant failure in the more severe cases.[2] Therefore, to improve the performance of metallic implants, surface functionalization with biologically active molecules has efficiently been exploited to address both problems. As an example, the presence of adhesive extracellular matrix (ECM) proteins on the surfaces, such as collagen and fibrinogen, or direct signaling proteins, such as bone morphogenic protein (BMP-2), was exploited to ensure an increasing osseointegration. Indeed, the ECM proteins promote the adhesion and colonization of the surfaces by stem cells. BMP-2 proteins increase the rate of bone formation by accelerating the differentiation and mineralization of the adherent cells.[3] Similarly, antimicrobial molecules such as the nisin peptide[4] or the dispersin B enzyme[5] were successfully included on the surface to promote bacteria contact-killing properties and prevent biofilm formation, respectively.

To promote long-lasting surface performances, the permanent anchoring of biomolecules is generally favored over adsorption methods. Such an approach implies the presence of chemically reactive sites on the surface of the materials that are able to interact with the biomolecule-containing functional groups.[6] More important, it is worth noting that the covalent immobilization of bioactive biomolecules on the surface still represents a technological challenge, requiring, among other conditions, the control of the functional group density available on the surface and the non-denaturation of the immobilized biomolecule.[7] Indeed, the amount of immobilized biomolecules on the material surface is critical for the expression of their functions in a specific environment. Therefore, the functional surface group density appears as a key parameter. Both insufficient and excessive functional group densities might lead to biologically inactive surfaces due to a poor amount of immobilized biomolecules and likely multianchoring processes, respectively. In addition, the biomolecule is generally immobilized through a random configuration, which might induce a loss of the biological activity.

In this quest for the production of optimized biomaterials, the successful pioneer strategy relying on a single biomolecule immobilization has been progressively replaced in favor of a multifunctional strategy. This latter approach is based on the immobilization of a cocktail of biomolecules, thus implicitly complexifying the issue related to biomolecule immobilization.[8]

Various routes are already reported for the multifunctionalization of surfaces, namely (a) the successive immersion, generally in overestimated durations, of a single surface in different biomolecule-containing solutions[9]; (b) the single immersion of a surface in a solution containing a mixture of biomolecules[10]; and (c) the immobilization of synthetic and multifunctional biomolecules, also known as fusion proteins.[11]

More importantly, most biomaterial surfaces lack chemical reactive sites, thus limiting their potential for biomolecule covalent modifications toward the development of functional coatings. Since the pioneering work of Messermith,[12] polydopamine coating has massively been exploited to fabricate multifunctional substrates.[13,14] Indeed, dopamine can easily self-polymerize in a buffered solution at pH 8.5, thus coating virtually any kind of inorganic and organic surfaces. Furthermore, by using a simple dipping process, the polymerized layer enriched in quinone groups enables the covalent immobilization of thiol- or amine-based biomolecules via Schiff base or Michael additions.[15]

From the laboratory to the industry scale, atmospheric pressure plasma polymerization has received considerable attention for its ability to produce high purity functional organic coatings, known as plasma polymer films (PPFs), in solvent and catalyst-free conditions. Hence, various atmospheric-deposited PPF-containing carboxylic,[4] amino,[16] epoxy,[17] and, more recently, catechol/quinone groups[18] have already been successfully exploited for the covalent immobilization of biomolecules. As an alternative to the polydopamine approach, we reported an atmospheric pressure liquid-assisted plasma polymerization technique (AP-LAPP) for the fast deposition on smooth and rough 2D titanium substrates of poly(methacrylate) films bearing catechol/quinone moieties for the single immobilization of bioactive molecules.[19,20] Interestingly, the AP-LAPP technique presents the advantage of operating with liquids having a lower vapor pressure than needed for the vapor transport in plasma-enhanced chemical vapor deposition setups. Hence, such an approach has successfully been exploited for the production of antibiofouling surfaces from hydroxyethylmethacrylate[21] and solid SiO_x films from siloxane-based liquid precursors.[22]

In this study, we report the facile and efficient immobilization of two complementary biomolecules on atmospheric pressure liquid-assisted plasma-polymerized

films. The fast and facile dipping of PPFs in a sodium periodate solution oxidizes the catechol-bearing PPFs to quinone groups and enables them to increase the amount of immobilized biomolecules. In the first section of this study, the influence of the sodium periodate-mediated oxidative reaction on the chemical and morphological properties of the plasma-deposited films is thoroughly investigated by using an analytical multitool approach combining atomic force microscopy (AFM), Fourier-transform infrared spectroscopy, ultraviolet, and X-ray photoelectron spectroscopy (XPS) measurements. The potency of the approach is validated by immobilizing a Ranaspumin-2 recombinant (Rsn) protein or lysozyme, with all characterization tools demonstrating their grafting and biological activity once immobilized separately on the surface. Finally, the controlled co-immobilization of lysozyme and Rsn is carried out, leading to promising multifunctional surfaces.

2 | EXPERIMENTAL

2.1 | Materials

A home-synthesized catechol containing methyl 3-(3,4-dihydroxyphenyl)-2-(2-methylprop-2-enamide) propanoate (DOMAm) was provided by Symbiose Biomaterials (Belgium). Methyl methacrylate (MMA, 99%), ethylene glycol dimethacrylate (EGDMA; 98%), sodium (*meta*)periodate (ReagentPlus®, 99%), sodium acetate, acetic acid, bovine serum albumin (BSA, ≥96%), Decon90 agent, lysozyme (hereafter noted as Lsz, ≥95% [L6876], 14.3 kDa, 3.39 nm), and *Micrococcus lysodeikticus* bacterium (M3770), which was a part of the Lysozyme Detection Kit (LY0100), were purchased from Sigma-Aldrich and used as received. Acetone, ethanol (technical grade), phosphate-buffered saline (PBS), and Dulbecco's phosphate-buffered saline (DPBS, 1×) solutions were acquired from VWR International. A recombinant protein of the biosurfactant Ranaspumin-2 (hereafter noted as Rsn, 13.6 kDa, 3.34 nm) was produced and purified by MBPEL (Belgium). The Rsn biomolecule presents a cleavable hexahistidine tag and a C-terminal cysteine, and it is known to promote bioconjugation reactions with quinone-functionalized surfaces via a Schiff base formation and Michael addition reactions, respectively.[23,24] To promote the site-specific attachment of the Rsn, the biomolecule immobilization was carried out at pH 8.5. Indeed at this pH, the sulfur atom is deprotonated, forming a thiol anion, a highly nucleophilic group reacting easily with electrophiles.

Silicon wafers (Siegert Wafer), mirror-polished 304-8ND stainless steel discs (SS; 2-cm diameter and 0.8-mm thickness; Aperam), 35-nm titanium physical vapor deposition-coated Au-QCM-D sensors (Quartz Pro AB), and etched titanium discs (provided by Nobil Bio Ricerche) were used as substrates. The substrates were cleaned according to successive ultrasonic washings in Decon90 (2 vol%) solution (5 min), MilliQ water (1 min), acetone (three times, 5 min), and pure ethanol (three times, 5 min), and further dried under a nitrogen flux. In addition, before plasma deposition, all substrates were activated, owing to a 30-s Ar:O_2 plasma treatment (19:1 L/min) ignited by a 10-kHz sinusoidal electrical excitation (SOFTAL generator) operating at 1.6-W/cm^2 in a continuous mode.

2.2 | Film characterizations

AFM images were obtained with a PicoLE microscope (Molecular Imaging) in air at scan rates between 0.5 and 1 Hz. Topography data were obtained via height channel using a semi-contact silicon cantilever (HQ:NSC15; MikroMasch) and a spring constant of 40 N/m. Images were captured by the SPIP software (ImageMet).

FTIR spectra of the plasma-deposited films on SS discs were acquired in the 800–4,000 cm^{-1} range at a 4 cm^{-1} resolution using a Bruker Hyperion 2000 microscope equipped with a grazing angle objective.

PerkinElmer Lambda 950 UV/Vis/NIR Spectrophotometer with 100-mm sphere and PMT/InGaAs detector (861 nm, 2 nm slit) were used to record UV/Vis scans in the 200–800 nm range.

XPS analysis was carried out using an Escalab 250Xi (Thermo Fisher Scientific) instrument equipped with an electron flood gun for insulators. These measurements were carried out at pass energy of 200 and 20 eV for the survey and narrow scan acquisitions, respectively. Quantifications were carried out by using the sensitive factor library provided by the manufacturer. Data processing was done using CASA XPS software (Casa Ltd., UK).

2.3 | AP-LAPP technique

Liquid-assisted plasma deposition was carried out using an AP dielectric barrier discharge process. Briefly, the process is composed of two flat high-voltage electrodes covered with alumina, ensuring an efficient plasma surface zone of 18.72 cm^2. A 20-L/min argon flow was used to feed the plasma discharge ignited by a 10-kHz sinusoidal signal and a 1.6 W/cm^2 power density. The upper smooth parts of the substrates were mounted on a mobile table acting as a grounded electrode. The precursor mixture, composed of a 2-mg/ml DOMAm-containing

MMA:EGDMA solution (99.8:0.2 molar%), was first sprayed on the substrates using a 48-kHz ultrasonic atomizing nozzle (2.9 W; Sono-Tek Corporation) supplied with a 0.1-ml/min flow by using a syringe driver. At the output of the nozzle, a 5-L/min nitrogen flow was used to shape the mist and direct it on the substrate surfaces. Hence, in the second step, the film synthesis occurred by exposing the prepared surface to the plasma zone. The table speed and the gap between the electrodes were set at 100 mm/s and 1 mm, respectively. The coating thickness was fixed at 90 (±10) nm.

2.4 | Oxidative reaction of the plasma-coated substrates

According to the procedure reported by Weidman,[25] plasma-coated substrates were oxidized via immersion for 5 min in a 50-mmol acetate buffer solution containing 0.05-g/ml $NaIO_4$ at pH 4. Surfaces were rinsed by dipping 10 times in acetate buffer at pH 4.

2.5 | Ranaspumin immobilizations on coated substrates

The bioengineered Ranaspumin was immobilized on coated substrates to confer them antibiofouling properties. The immobilization conditions were 1-mg/ml Rsn in DPBS at 10 mM, pH 8.5, for 1 hr at room temperature.[20] Unbound biomolecules were eliminated after three successive washes of 5 min each, with a stirring speed under 250 rpm, using first DPBS and then MilliQ water.

2.6 | Lysozyme immobilization on coated substrates

Lysozyme was immobilized on plasma-coated substrates using PBS 0.5 M at pH 7.4 according to the procedure reported by Meslmani et al.[26] Indeed, such buffer pH value ensures that amino-bearing Lsz is in its deprotonated form and thus able to undergo nucleophilic attack on quinone-functionalized surfaces. In addition, such a neutral pH for Lsz bioconjugation was reported to ensure its optimal antibacterial activity. Also, five different Lsz concentrations, varying from 0.001 to 10 mg/ml, were investigated. Lsz grafting was carried out at 22°C. Unreacted Lsz was removed via three successive rinsing steps with PBS and MilliQ water under gentle agitation (250 rpm) for 5 min.

2.7 | Investigation of the biomolecule immobilization reactions by quartz crystal microbalance with dissipation monitoring (QCM-D)

Real-time immobilization of Lsz and Rsn GC tag biomolecules on the surface of plasma-coated sensors (Ti X-cut resonators with a 4.95-MHz resonant frequency) was investigated by the QCM-D technique using a QSense Explorer System (QSense; Biolin Scientific). Data retreatment was carried out using the QSense Software QTools. For all experiments, the PBS solution flow rate was fixed at 100 µl/min, and the system allowed to equilibrate, achieving a stable baseline. The pH of the buffered solution was fixed at 7.4 or 8.5, when using Lsz and Rsn, respectively. The monitored frequency (Δf) provides insight into the mass of adsorbed biomolecule. In particular, the quantity of mass absorbed on the surface was estimated, with nanogram precision sensitivity (i.e., 0.5 ng/cm), according to the Sauerbrey equation[27]:

$$\Delta m = -\frac{\rho \times l}{f0 \times n} \times \Delta f = -C \times \Delta f, \quad (1)$$

where Δm is the mass absorbed, Δf is the frequency change, n is the harmonic number, ρ and l are the density and thickness of quartz, respectively, and $f0$ is the fundamental resonant frequency. For a 5-MHz resonator, as used here, the mass sensitivity constant, C, is equal to 17.7 $ng \cdot cm^{-2} \cdot Hz^{-1}$.[28] The biomolecule saturation time might be estimated as the time value corresponding to the intersection point between the frequency shift plateau achieved after the PBS rinsing step (i.e., removal of the unbonded molecules) and the frequency shift curve.

2.8 | Evaluation of the antimicrobial activity

The activity of Lsz was assessed using a similar procedure reported by Conte et al.[29] Briefly, it consists of using *M. lysodeikticus* as a model microbial species. An initial suspension of *M. lysodeikticus* 0.01% (w/v) was prepared in PBS (0.1 M, pH 6.8 at room temperature) and diluted to obtain a final cell suspension with an absorbance at 450 nm between 0.6 and 0.7 versus PBS, in accordance with the manufacturer's instruction. Nonbioconjugated (controls) and bioconjugated samples were kept in contact with 7 ml of the bacteria suspension in a six-well plate (sterile, nontreated; VWR International). The antimicrobial activity was determined by monitoring the decrease in absorbance at 450 nm (A_{450}) using the

spectrophotometer Spark 20 M (Tecan), resulting from the cellular lysis of the bacteria. The samples were continuously in contact with the stirred microbial suspension (150 rpm, humid atmosphere, room temperature). A_{450} was monitored until a plateau of value was reached. Each test was carried out in triplicate. To quantitatively determine the antimicrobial activity from the absorbance data, the Gompertz–Zwietering equation was used:

$$\bar{A}_t = A_0 + A\exp\left\{-\exp\left[\frac{d_{\max} e}{A}(\lambda - t) + 1\right]\right\}, \quad (2)$$

where $\bar{A}(t)$ is the normalized absorbance at time t (i.e., obtained by dividing the absorbance at t by the initial absorbance), A_0 corresponds to the initial value of $A(t)$ and generally close to 1, A is the difference between K and the lower asymptote of the absorbance curve, $d_{\max}$ is the maximum absorbance decrease rate, defined as the tangent at the inflexion point and expressed as the rate per second, λ is the lag phase (in seconds), and t is the time (in seconds).

Experimental absorbance data were fitted using Equation (2) and the $d_{\max}$ value was taken as a quantitative measure of the antibacterial activity of all surfaces tested.

As a complementary test to evaluate the antimicrobial activity, colony-forming units of *M. lysodeikticus* (CFU/ml) were analyzed by membrane filtration (GN-6 Metricel Membrane, 0.45 μm; Pall) on a Tryptone Soy Agar Plate (30°C, 48 hr). Initial suspensions of *M. lysodeikticus* (optical density [OD] at 450 nm = 0.7) with a cell concentration of 3×10^7 CFU/ml in a PBS were treated using free Lsz, leading to suspensions with different final OD values. By correlating OD values with bacteria concentrations, the antibacterial activity was expressed in log reduction.

2.9 | The evaluation of the antifouling activity of the surfaces

Protein adsorption on bare, plasma-coated, and bioconjugated titanium-coated QCM-D sensors was measured by QCM-D using a 100 μl of 1-mg/ml BSA solution. The evaluation of the data was performed with the QTools software (QSense).

2.10 | Biocompatibility assessment via MG-63 cell culture

Etched titanium disks were firstly cleaned with a 2% RBS cleaning solution and rinsed with PBS (1x) and MilliQ water (4x). Then, after ultrasonic cleaning in a 80% ethanol (2x, 10min.), each face of the substrates were UV-sterilized for 30 min. All manipulations were carried out under sterile conditions (L2 laminar flow hood). The cells were cultured under the condition of 5% CO_2 and 37°C (Binder incubator, Tuttlingen, Germany). In total, 48-well black plates with lid (In Vitro Scientific) were used and polystyrene (PS) culture wells (CD) were seeded as a reference positive control. Three discs were prepared for each condition and the experiment was carried out in two replicates. All wells were rinsed with a 0.5-ml physiological PBS solution and then 0.5-ml complete culture medium, and they were incubated for 30 min within a CO_2 incubator. The culture media was composed of Dulbecco's modified Eagle's medium (DMEM) high glucose, GlutaMAX™ Supplement, pyruvate (31966-021 Gibco; Invitrogen, Paisley, UK) supplemented with 10% inactivated fetal bovine serum (Gibco), 100 IU/ml penicillin and 100 μg/ml streptomycin (Lonza Verviers, Belgium). Also, 5,000 MG-63 (mycoplasma-free) cell lines were seeded per well in a 0.5-ml complete medium.

To evaluate the living cell population under different conditions, a viability test was then performed directly on discs for 72 hr. Cellular viability of 100% was attributed to the MG-63 grown in control PS wells without disc samples. Cellular viability was quantified by a colorimetric assay using 3-(4,5-dimethylthiazol-2-yl)-5-(3-carboxymethoxyphenyl)-2-(4-sulfophenyl)-2*H*-tetrazolium (inner salt MTS; Promega, Madison). MTS solutions were prepared according to the manufacturer's instructions. Discs were rinsed with 0.5 ml of DMEM/F-12 (Gibco), and 0.5 ml of new DMEM/F-12 with MTS solution (10%) was applied. The plates were incubated at 37°C in the absence of light for 45 min. Then, the plates were shaken for 3 min. Furthermore, 200 μl of supernatant was removed from each well and placed in 96-well microplates. The absorbance of supernatant aliquots was read at 492 nm using the PowerWave X microplate spectrophotometer (BioTek instrument Inc., Winooski, VT), and the viability was calculated and normalized from the absorbance of control samples taken as 100% (PS). Immunofluorescence staining was conducted on the same samples after the MTS assays. Discs were rinsed two times with 0.5-ml PBS and the cells were fixed with 4% paraformaldehyde (Sigma-Aldrich) in PBS at room temperature for 20 min. Immunostaining was then performed. Cell permeabilization was performed with 0.5-ml, 0.5%, Triton X-100 (Sigma-Aldrich) at 4°C for 20 min. Blocking was performed with 1% BSA (Sigma-Aldrich) in PBS at 37°C for 30 min. Vinculin was stained with mouse anti-vinculin (V9131; Sigma-Aldrich) and rabbit anti-mouse Alexa Fluor 568 (Life Technologies, Carlsbad, CA); the incubation was performed in PBS solution with corresponding dilutions (1:200) at 37°C for 1 hr for mouse anti-vinculin and at room temperature or 30 min for rabbit anti-mouse Alexa Fluor 568. Actin was stained by incubating in PBS solution with 1:40 dilution of Alexa Fluor 488-labeled phalloidin (Life Technologies) at 37°C for 1 hr. A nuclear

stain dye DAPI (4′,6-diamidino-2-phenylindole dihydrochloride; D8417-1MG; Sigma-Aldrich)/PBS 1:5,000 was added and allowed to set at room temperature for 10 min. The stained sample surface was observed with an IX81 optical inverted microscope equipped with a UPlanFL objective at ×20 magnification and with an XCite-iris IX fluorescence unit and a C-BUN-FXC50 charge-coupled device camera (Olympus Optical Co., Ltd.). A qualitative analysis of cellular morphology on discs was conducted with the fluorescent actin, DAPI, and vinculin staining for 72 hr.

3 | RESULTS AND DISCUSSION

3.1 | Atmospheric liquid-assisted plasma polymerization and oxidative reaction to produce quinone-bearing coatings

By using the atmospheric liquid-assisted plasma polymerization technique depicted in Figure 1, etched titanium surfaces, SS, silicon wafers substrates, and titanium-coated QCM-D sensors were successfully coated with a catechol-functionalized layer, hereafter noted as pp(layer).[20,30]

According to AFM analysis (Figure 2a), the deposited layer covered the entire surface of the substrate and was pinhole-free. The surface was also smooth with an arithmetical mean height roughness (Sa) of about 0.25 nm. The UV analysis, reported in Figure 2c, appeared as a key technique confirming the presence of catechol groups in the deposited film due to the appearance of the UV peak at 280 nm.[31] The IR analysis, shown in Figure 2d, confirmed the methacrylate-based matrix composing the coating, with C═O and C–O–C ester bands at 1,736 and 1,148 cm^{-1}, respectively. The good incorporation of the catechol-based monomer was related to the detection of the C═O, N–H, and C–N amide bands located at 1,660, 1,511, and 1,260 cm^{-1}, respectively.[20]

To gain insight into the surface chemistry of the films, XPS analyses were carried out. The curve fitting of the XPS C1s core level of the pp(layer), reported in Figure 3a, highlighted a poly(methyl methacrylate)-like surface with the presence of the characteristic contributions related to unsaturated carbon at 285 eV, secondary carbon in ester at 285.8 eV, carbon–oxygen at 286.6 eV, and carboxyl group in ester at 289.1 eV. Interestingly, compared with the poly(methyl methacrylate) C1s curve fit,[32] an additional contribution at 287.7 eV, related to the amide group, was detected in accordance with the N1s XPS curve fitted with a single contribution at 400 eV (Figure 3c). Such results were in agreement with the IR results, suggesting the incorporation of the DOMAm inside a methacrylate-based matrix. However, compared to the C1s spectra of the polydopamine,[33] it could be noted that any π–π* shake-up peak at 291.1 eV, arising from the excitation of the π orbital, was observed. This suggested an inferior catechol content in the plasma-deposited film.

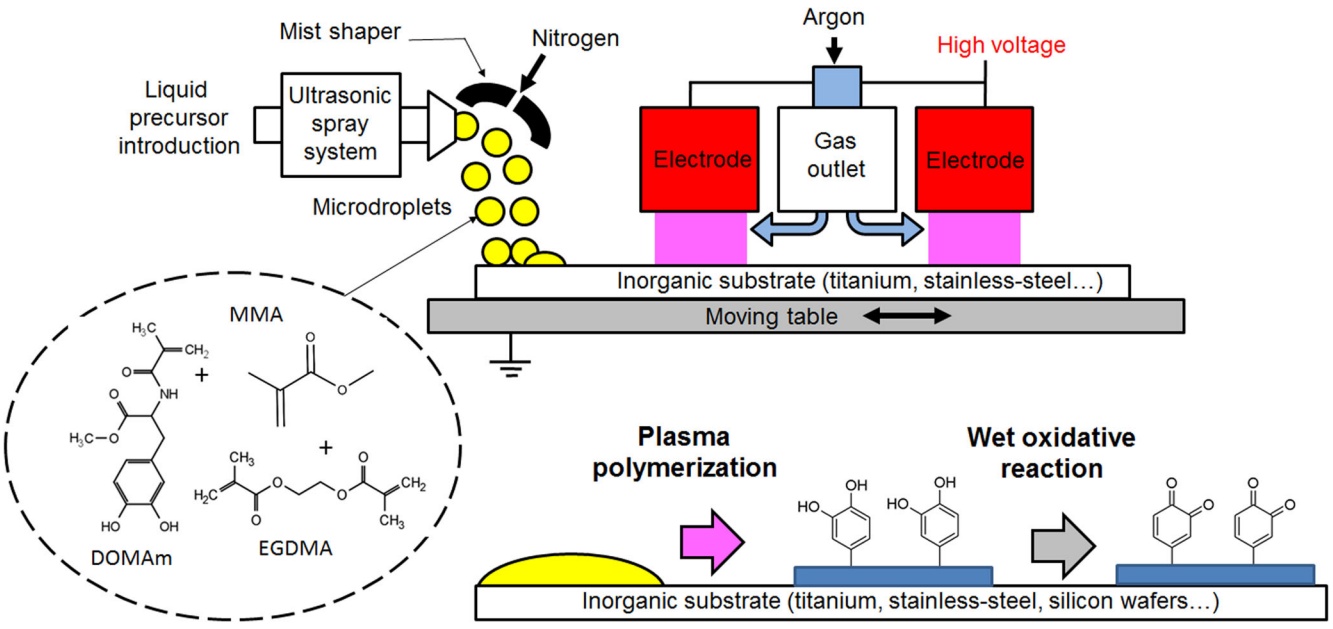

FIGURE 1 A scheme of the atmospheric liquid-assisted plasma technique to deposit catechol-functionalized coatings and their subsequent oxidation to quinone-bearing coatings. DOMAm, methyl 3-(3,4-dihydroxyphenyl)-2-(2-methylprop-2-enamide) propanoate; EGDMA, ethylene glycol dimethacrylate; MMA, methyl methacrylate

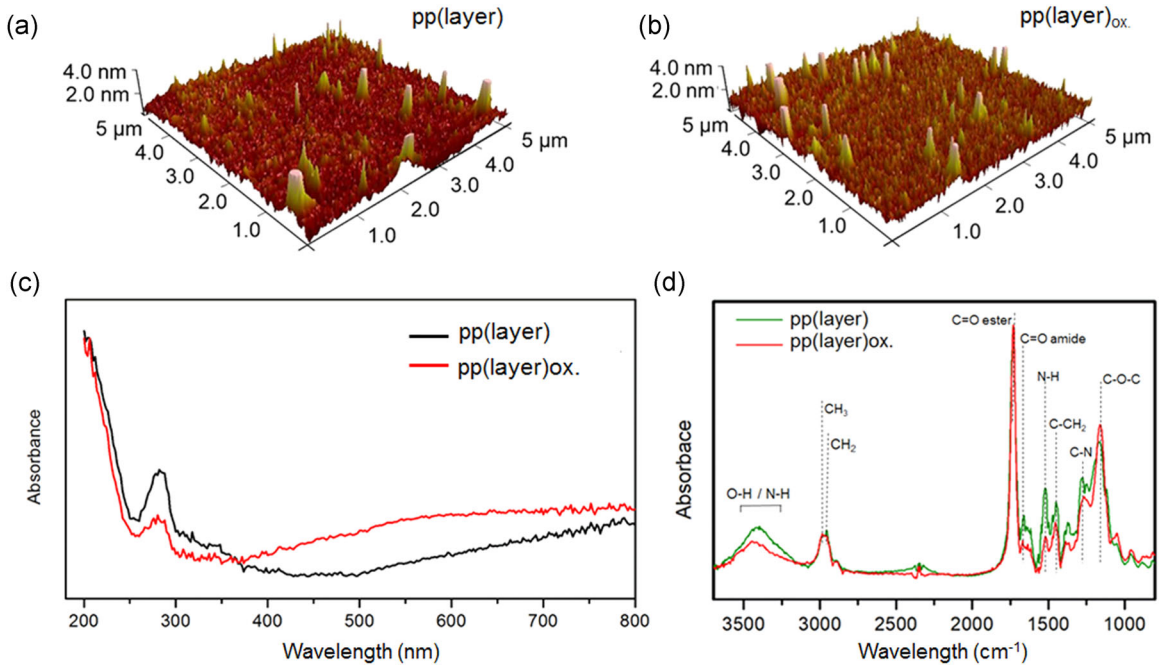

FIGURE 2 Coating characterizations. (a) Atomic force microscopy pictures of pp(layer) and (b) pp(layer)ox. deposited on silicon substrate, (c) ultraviolet spectra of pp(layer) and pp(layer)ox. deposited on stainless steel discs, and (d) infrared spectra of pp(layer) and pp(layer)ox. deposited on stainless steel discs

To produce quinone-bearing films, the as-deposited layers were subsequently oxidized by dipping for 5 min in a periodate solution. The resulting layer, hereafter noted as pp(layer)ox., presented a smooth roughness (Sa ~0.3 nm; Figure 2b). The successful oxidative reaction was confirmed by the UV analysis (Figure 2c), with the sharp decrease of the catechol peak at 280 nm along with the increase of the quinone peak around 395 nm. However, the presence of a residual catechol peak suggested an incomplete catechol moieties conversion in the entire bulk of the layer. Finally, from the IR analysis (Figure 2d) and the C1s (Figure 3d), according to the XPS sensitivity, it appeared that pp (layer) and pp(layer)ox. presented similar surface compositions with C:N:O values equal to 71:2:27 and 71:2.5:26.5, respectively. With XPS curve fitting, it was possible to conclude that after the oxidation step, the layer still preserved its polymethacrylate-based matrix composition with the presence of DOMAm units, as suggested by the XPS N1s core level data (Figure 3f). Finally, by comparing the O1s curve fits of the coating before and after the oxidation step (Figures 3b and 3e), two main contributions, namely the ester/amide/quinone contribution at 532.3 eV and the carbonyl/catechol contribution at 533.6 eV, were detected. These presented similar surface areas, thus preventing any monitoring of the catechol conversion into quinone by XPS analyses.

3.2 | Ranaspumin immobilization on quinone-bearing coatings and preliminary cytotoxicity tests

To investigate the relevance of the oxidative reaction, a bioengineered Ranaspumin (Rsn) was immobilized (at 1 mg/ml, PBS at pH 8.5) on as-deposited and oxidized layers for different periods of time. The modified surfaces were analyzed by XPS analyses, and the detected N1s element (fingerprint of Rsn due to its presence in its amino acid sequence) was monitored and quantified. As shown in Figure 4, irrespective of the immobilization duration (up to 2 hr), higher amounts of Rsn are systematically immobilized on oxidized layers, thus confirming the relevance of the oxidative step. In addition, it is worth noting that, irrespective of the coating nature, surfaces are saturated by Rsn in approximately 10 min.

From QCM-D measurements shown in Figure 5a, it was concluded that the Rsn grafting kinetic was fast, with a surface saturation achieved in 8 min. Hence, compared with XPS analyses (Figure 4), QCM-D appeared as a more accurate technique to estimate the optimized grafting duration, that is, an abscissa value of the final frequency considering the rinsing step. More importantly, the successful immobilization of biomolecule on surfaces should not be considered as the successful production of active surfaces, as specific conformations or orientations of the biomolecule should be preserved. Therefore, here, to

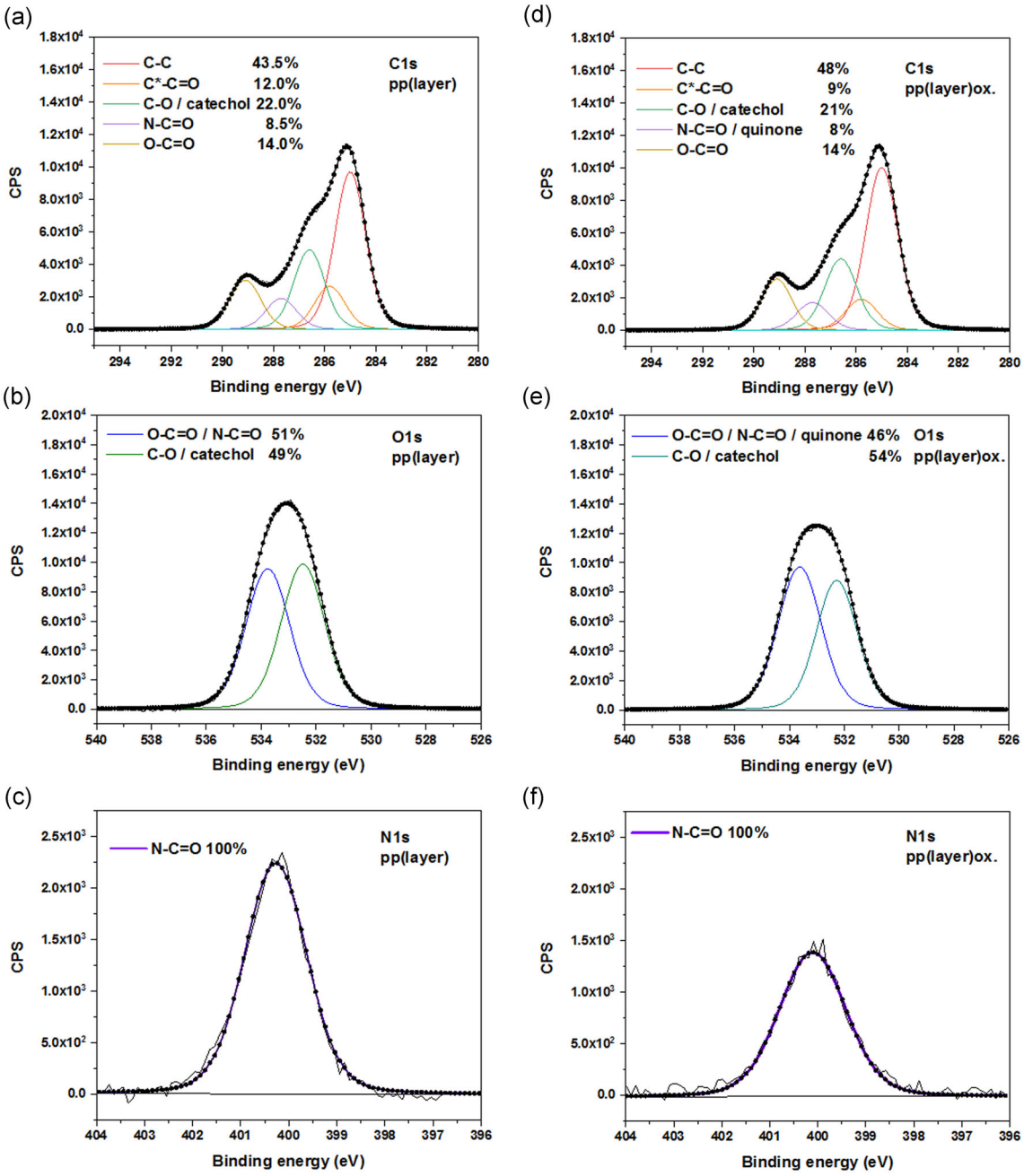

FIGURE 3 X-ray photoelectron spectroscopy curve fittings. (a) C1s curve fits of pp(layer) and (d) pp(layer)ox., (b) O1s curve fits of pp(layer) and (e) pp(layer)ox., (c) N1s curve fits of pp(layer) and (f) pp(layer)ox

investigate the antifouling properties of the produced surfaces, the interactions of BSA, known as a fouling protein, and Rsn immobilized on plasma-coated Ti-QCM-D sensor were investigated via QCM-D measurements. For the sake of comparison, BSA interactions with bare and pp(layer)ox.-coated sensor were also studied. From Figure 5b, reporting the frequency (Δf) shifts during the protein adsorption, it appeared that pristine smooth titanium surfaces promoted the absorption of a significant amount of BSA, estimated at around 496.5 ng/cm^2 according to the Sauerbrey model. Interestingly, compared with bare titanium surface, the oxidized PPF presented an antifouling property, with a lower amount of BSA adsorbed at its surface (i.e., 298 ng/cm^2). Such a result might be explained by the hydrophilic character of the oxidized film (i.e., water contact angle values were estimated at $59.6 \pm 0.8°$), thus limiting hydrophobic protein–surface interactions. Finally, it was observed that Rsn-immobilized surfaces allowed to efficiently prevent any BSA attachment, as barely any

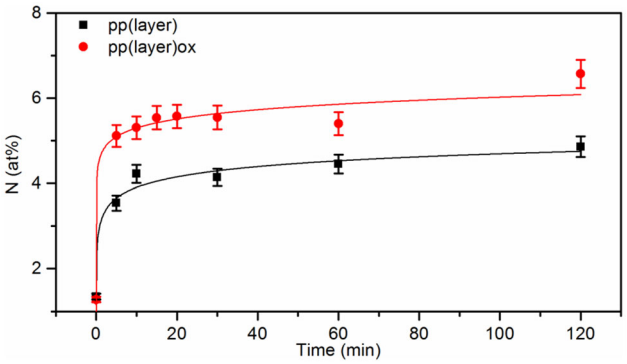

FIGURE 4 The evolution of the N1s X-ray photoelectron spectroscopy content on pp(layer) and pp(layer)ox. deposited on silicon substrates after Ranaspumin immobilization with different immobilization durations

frequency shift variation is recorded. More importantly, despite the fact that the plasma-deposited film contained an inferior content of catechol groups compared with polydopamine coating, it can be observed that the quinone surface density was high enough to efficiently immobilize Rsn for producing antifouling surfaces.

As the Rsn is a bioengineered protein, preliminary in vitro biological tests have been carried out to evaluate its cytotoxicity for potential biomedical applications. For this, MG-63 cells were cultured on etched titanium surfaces, without or with adsorbed Rsn. Osteoblastic responses in vitro are widely used before developing in vivo studies,[34] and human preosteoblastic MG-63 cell line is one of the common interesting cell lines to investigate the osteoblastic response to biomaterials contamination.[35] In this study, viability and adhesion properties were evaluated on the Rsn-modified surfaces. As reported in Figure 6, viability percentages were not significantly modified with MTS (93% with regard to etched Ti taken as 100%). In addition, the cell morphology study revealed that MG-63 cells were spread on the etched titanium surface with thin elongated filopodia, with or without adsorbed Rsn. Vinculin was positive in cytoplasm and in few focal contact points.

3.3 | Lysozyme immobilization onto quinone-bearing coatings

To investigate the influence of the lysozyme (Lsz) solution concentrations on the density of Lsz immobilized on the quinone-functionalized film, oxidized layers were immersed at 22°C for 1 hr in Lsz solutions at different concentrations, namely 0.1, 1, and 10 mg/ml. The XPS chemical compositions of the resulting surfaces are shown in Table 1. Irrespective of the Lsz concentrations, the modified surfaces presented an increased content in nitrogen and sulfur was detected. As N and S might be undoubtedly attributed to the Lsz amino acid sequence, XPS confirmed an efficient Lsz immobilization. However, as all the surfaces presented a similar composition, below the sensitivity limit of XPS for S, it was not possible to estimate the density of immobilized Lsz.

QCM-D experiments were carried out, as this technique is recognized for its efficiency in monitoring biomolecule–material surface interactions.[36] By recording the frequency shift, mass uptake, related to adsorbed biomolecules and water, might be estimated. More important, as a unique functional coating is exploited, the QCM-D technique can be considered, here, as a

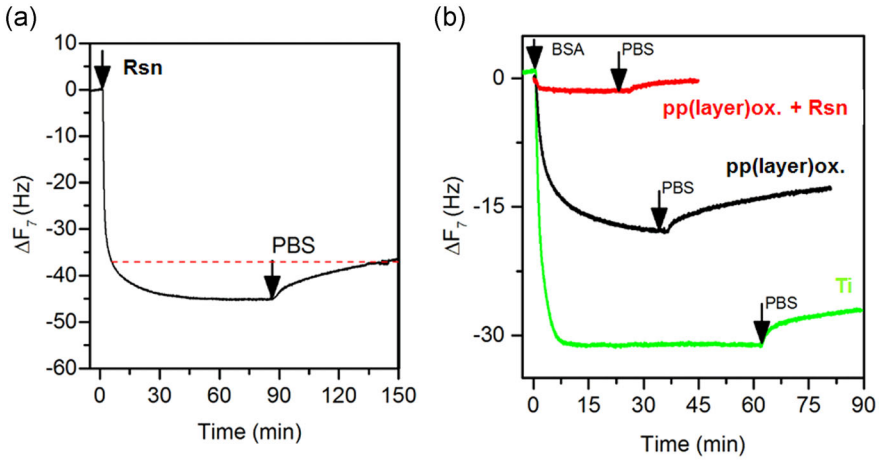

FIGURE 5 (a) ΔF plot for oxidized plasma polymer layer (pp(layer)ox.) deposited on a Ti-coated QCM-D sensor with 1-mg/ml Ranaspumin (Rsn) solution introduction at time 0, and (b) ΔF plots for pristine Ti-coated QCM-D sensor (green), pp(layer)ox. deposited on a Ti-coated QCM-D sensor (black), and Rsn immobilized on pp(layer)ox. deposited on a Ti-coated QCM-D sensor (red) with the introduction of bovine serum albumin at time 0. BSA, bovine serum albumin; PBS, phosphate-buffered saline; QCM-D, quartz crystal microbalance with dissipation monitoring

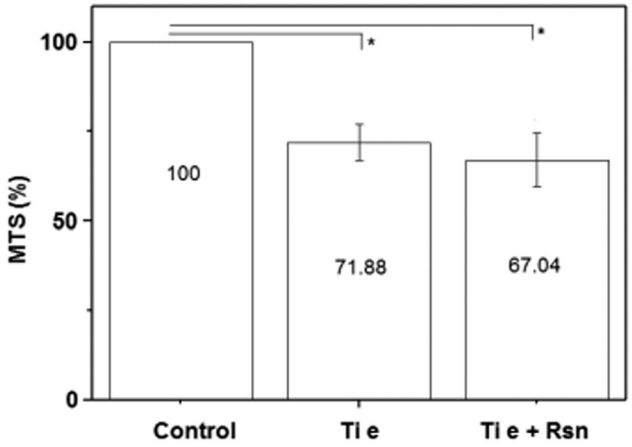

FIGURE 6 Viability of the MG-63 cells (MTS). Control etched titanium discs (Ti e), Ranaspumin (Rsn) adsorbed on etched titanium discs (Ti e + Rsn). (Kruskal–Wallis statistical test and Bonferroni multiple comparison; *significant [$p < .05$], [$n = 6$].)

discriminative method to estimate the optimal conditions for biomolecule adsorptions. Hence, frequency decrease is typically associated to mass increase. In addition, dissipation monitoring gives information on the viscoelastic property of the layer, with small dissipative values being associated to a rigid layer. Here, Ti-QCM-D sensors, first plasma-coated and subsequently oxidized, were placed in the QCM-D module at 22°C. Different Lsz solutions (at concentrations of 0.001, 1, 2.5, and 10 mg/ml) were injected on top of the coated sensor surface. This resulted in difference maximum frequency changes of the sensor caused by immobilized Lsz, as shown in Figure 7a. It appears that using a 0.001-g/m Lsz solution did not contribute to the biomolecule immobilization, as no frequency change was barely noticeable. An increase in concentration from 0.1 up to 10 mg/ml was accompanied by a decrease in the frequency shift, related to the Lsz adsorption on the surface. A significant diminution, from −15 to −45 Hz, was noticeable when increasing the concentration from 0.1 to 1 mg/ml. Interestingly, 1 hr of solution injections with concentration superior or equal to 1 mg/ml led to a similar frequency decrease, suggesting that comparable amounts of Lsz were adsorbed on the surface. This result was fully confirmed by applying the Sauerbrey equation, as a negligible dissipation shift was monitored. Indeed, as reported in Figure 7b, by taking into account the rinsing step, allowing to remove nongrafted Lsz, it was estimated that the optimal amount of immobilized Lsz was around 600 ng/cm^2. Interestingly, an Lsz concentration of 1 or 2.5 mg/ml resulted in a complete Lsz surface saturation in 30 min. In addition, by increasing the concentration by a factor of 10 (i.e., 10 mg/ml), it was noticeable that the kinetics of grafting was divided by a factor of 2, leading to a surface saturation in only 15 min.

TABLE 1 XPS atomic surface composition of stainless steel discs coated with an oxidized plasma layer before and after immersion in Lsz solutions at 22°C, for 1 hr, at different Lsz concentrations

	XPS atomic surface composition (at%)			
Substrates	**C**	**O**	**N**	**S**
pp(layer)ox.	70	26.5	3.5	–
Lsz-0.1 mg/ml	67.5	23.0	9.0	<0.5
Lsz-1 mg/ml	66.5	23.0	10.0	<0.5
Lsz-10 mg/ml	67.5	24.0	8.0	<0.5
Lsz (theory)	61.0	19.0	19	1

Abbreviations: Lsz, lysozyme; XPS, X-ray photoelectron spectroscopy.

To discriminate the different processed surfaces, the antibacterial surface activity was evaluated via the immersion of the substrates in a *M. lysodeikticus* solution. The lysis of the bacteria cells was evaluated from the decrease of absorbance measured at 450 nm (A_{450}). By applying the modified Gompertz equation, the A_{450} value was monitored as a function of time, as shown in Figure 8a, reporting the results for pristine surfaces (reference) and Lsz-immobilized surfaces during 1 hr with different concentrations. Interestingly, a good fitting of the experimental results to the model was achieved with a high coefficient of determination, R^2 (around 0.96).[25] In Figure 8b, the d_{max} values, denoting a key parameter corresponding to the maximal absorbance decrease rate and related to the antibacterial activity, are reported along with the results of the d_{max} statistical analysis. Hence, the pristine metallic surfaces did not present activity while effective antibacterial surfaces might be produced using Lsz-containing solutions with a concentration of 1 or 10 mg/ml. Interestingly, both Lsz concentrations lead to surfaces with a similar antibacterial activity ($p = .05$). Such a result was in agreement with the QCM-D measurements, highlighting a similar amount of immobilized Lsz by using these concentrations. Finally, according to the OD–bacteria concentration calibration curves (as described in the Section 2), Lsz surfaces grafted at 1 mg/L in 1 hr presented an antibacterial activity equivalent to a log reduction of 2.4.

By considering QCM-D and antibacterial results, it has been demonstrated that Lsz can be efficiently immobilized on quinone-bearing surfaces while conserving its antibacterial activity. In particular, using a 1-mg/ml Lsz solution at 22°C allowed saturating the surface in 30 min. Therefore, it might be assumed that Lsz immobilization reaction limited to 10 min might preserve some free quinone groups available for the subsequent grafting of another biomolecule.

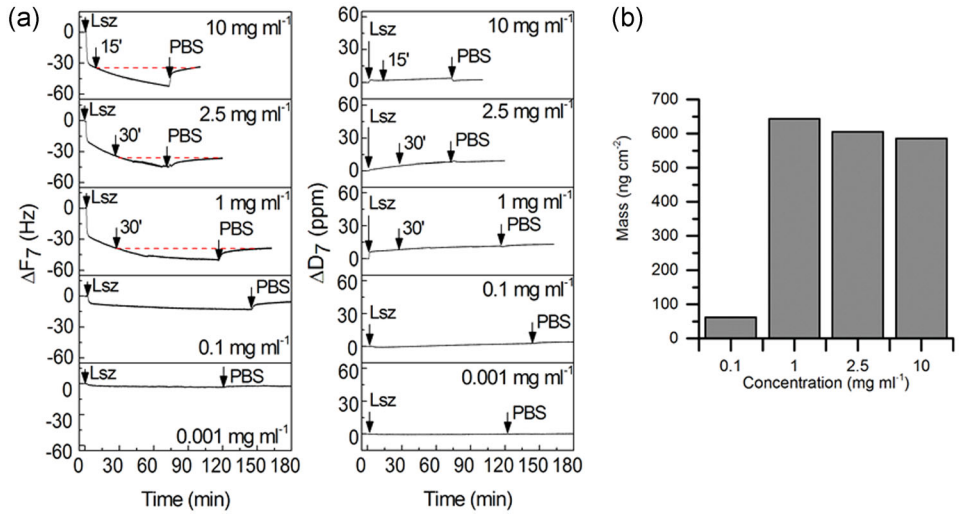

FIGURE 7 (a) ΔF and ΔD plots of oxidized plasma polymer layers deposited on Ti-coated quartz crystal microbalance with dissipation monitoring sensors with lysozyme (Lsz) solution introduction at time 0 for concentrations of 0.001, 0.1, 1, 2.5, and 10 mg/ml and (b) the amount of immobilized Lsz after 1 hr of reaction according to the Sauerbrey equation

In parallel, in vitro antibacterial tests confirmed that Rsn-immobilized surfaces presented a negligible antibacterial activity with a d_{max} value at around 0.5×10^{-6} (Figure 9b), thus confirming the necessity to immobilize Lsz to confer additional antibacterial activity to a surface.

3.4 | Dual Lsz and Rsn immobilization for multifunctional surfaces

Considering the different optimal pH of the Lsz and Rsn solutions, namely 7.4 and 8.1, Lsz and Rsn were co-immobilized on quinone-coated substrates via two successive dips, first in an Lsz solution at 1 mg/ml for 10 min and then in an Rsn solution at 1 mg/ml to saturate the surface. Figure 9a reports the different frequency changes during the alternative biomolecule introduction and rinsing steps. The systematic frequency decrease after Lsz and Rsn introduction indicated an increase in the wet adsorbed biomolecule mass at the coated sensor surface, thus confirming the successful biomolecule immobilization. As shown in Figure 9b, dual Rsn–Lsz-grafted surfaces presented an antibacterial activity, as the statistical test indicated nonsignificant difference

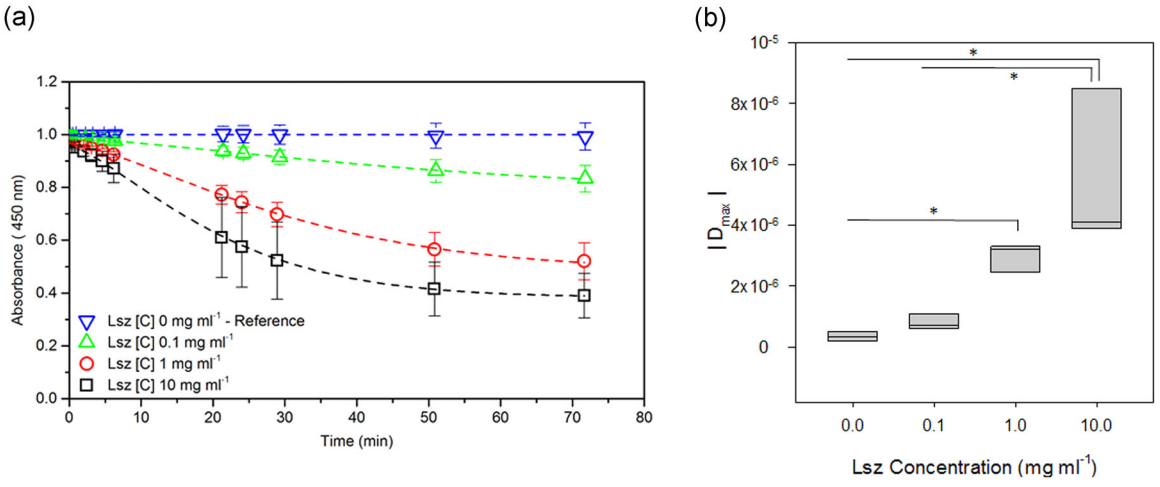

FIGURE 8 The efficacy of pp(layer)ox. deposited on stainless steel discs against *Micrococcus lysodeikticus* after grafting (1 hr) of lysozyme (Lsz) at different concentrations: 0 mg/ml (∇), 0.1 mg/ml (Δ), 1 mg/ml (O), 10 mg/ml (□). (a) The curves represent the fitting of the experimental data with the modified Gompertz equation, boxplots represent the absolute d_{max} values in function of Lsz concentration. (b) The median is represented for each box, and the dispersion of the data is indicated by the size of the box. (Kruskal–Wallis one-way analysis of variance on ranks ($p = .016$), followed by a pairwise multiple comparison [Student–Newman–Keuls method], *significant [$p < .05$], [$n = 3$].)

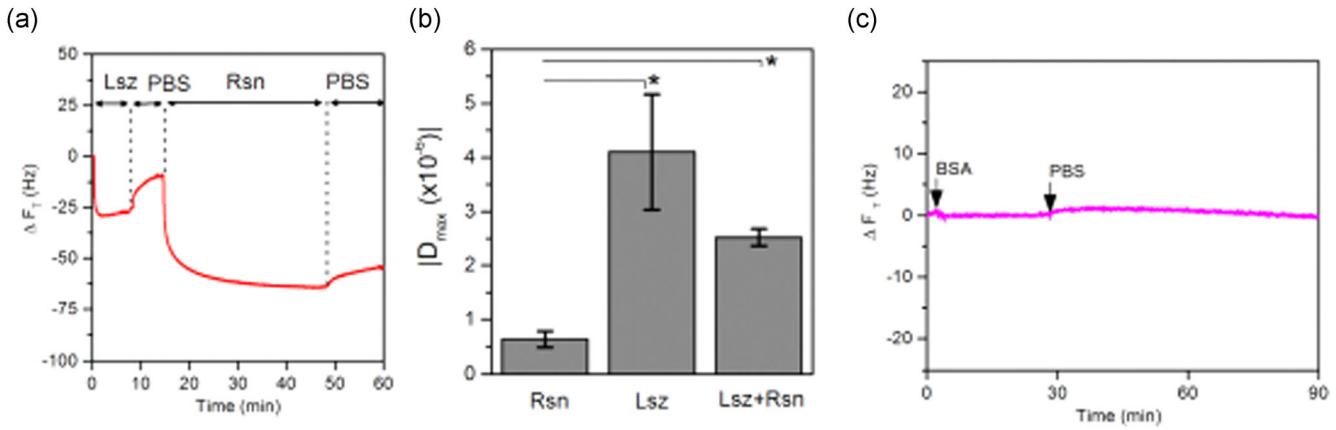

FIGURE 9 (a) The evolution of quartz crystal microbalance with dissipation monitoring (QCM-D) frequency shifts for oxidized plasma polymer layer deposited on a Ti-coated QCM-D sensor during lysozyme (Lsz) immobilization at 1 mg/ml for 10 min, phosphate-buffered saline rinsing, Ranaspumin (Rsn) immobilization at 1 mg/ml. (b) Absolute d_{max} values (mean and standard deviation) for oxidized layers deposited on stainless steels and subsequently bioconjugated with Rsn and Lsz, 1 mg/ml, for 10 min and Lsz–Rsn (1 mg/ml for 10 min and Rsn at 1 mg/ml for 60 min), one-way analysis of variance ($p = .002$), followed by a pairwise multiple comparison (Tukey's method), *significant ($p < .05$), ($n = 3$), (c) QCM-D frequency shifts for dual Lsz–Rsn immobilized on a pp(layer)ox coated Ti-QCM-D sensor with BSA introduction at time 0

($p = .05$) compared with Lsz-coated surfaces. Indeed, the surface remained active, with a log reduction estimated at 2.4. It was also concluded that the Rsn presence did not inhibit the Lsz action, probably due to its relatively small size (13.6 kDa) limiting steric hindrance phenomena. More importantly, the dual surfaces exhibited an outstanding antifouling property, as no BSA attachment was observed (Figure 9c), thus highlighting that the Lsz presence did not inhibit the Rsn biological action.

4 | CONCLUSION

In summary, quinone-bearing films were successfully deposited on metallic surfaces via a two-step procedure relying on an atmospheric liquid-assisted plasma deposition of catechol films and a sodium periodate-induced catechol oxidation in quinone groups. Such surfaces allowed facile bioconjugation of Lsz and/or Rsn in aqueous solutions at room temperature. Using QCM-D analyses, optimal Lsz grafting conditions including enzyme concentration and immobilization duration were determined (i.e., 22°C, pH 7.4, 1 mg/ml, 30 min). Similarly, the kinetics of the Rsn immobilization, carried out at pH 8.5 and 1 mg/ml, was estimated at 8 min. Finally, we were able to control the co-immobilization of Lsz and Rsn on the quinone-bearing films. Preliminary tests, carried out on the multifunctional surfaces, highlighted promising results with the detection of dual bactericidal and antifouling properties.

ACKNOWLEDGMENTS

The authors would like to thank Dr. J. Guillot from Luxembourg Institute of Science and Technology for his skillful XPS characterization and valuable discussions. Dr. M. Blique (dentist, Luxembourg), Dr. F. Lambert (head of clinic, CHU of Liège and associate professor in Dental Biomaterials, University of Liège, Belgium), and Prof. A. Mainjot, all members of the METABIO project advisory board, are gratefully acknowledged for fruitful discussions about dental implants and biomaterials. Finally, the authors would like to thank F. Cambroisier, from the University of Liege, for the cell culture studies. C. Detrembleur is FNRS Research Director, and the authors thank the National Fund for Scientific Research (Belgium) for funding. This study was carried out in the framework of the European M-ERA.NET METABIO (FNR INTER/MAT/13/13) and BIOREAFILM (C15/MS/10365992/BIOREAFILM/Moreno) projects funded by the Luxembourgish Agency "'Fonds National de la Recherche"' and the DG06-Région Wallonne Agency (METABIO/no. convention 111278 and 1318213).

ORCID

Urszula Czuba http://orcid.org/0000-0002-1179-2336
Maryline Moreno-Couranjou http://orcid.org/0000-0003-0041-5532
Marie-Claire De Pauw-Gillet http://orcid.org/0000-0002-9843-6894
Robert Quintana http://orcid.org/0000-0003-0879-053X
Patricia Lassaux http://orcid.org/0000-0002-2197-5443

Christophe Detrembleur http://orcid.org/0000-0001-7849-6796
Patrick Choquet http://orcid.org/0000-0001-8696-5812

REFERENCES

[1] M. Kaur, K. Singh, *Mater. Sci. Eng., C* **2019**, *102*, 844.
[2] K. Bazaka, M. V. Jacob, R. J. Crawford, E. P. Ivanova, *Appl. Microbiol. Biotechnol.* **2012**, *95*, 299.
[3] C. A. C. Stewart, B. Akhavan, J. Hung, S. Bao, J. Jang, S. G. Wise, M. M. M. Bilek, A. C. S. Biomater, *Sci. Eng.* **2018**, *4*, 4084.
[4] R. Mauchauffé, M. Moreno-Couranjou, N. D. Boscher, C. Van De Weerdt, A. Duwez, P. Choquet, *J. Mater. Chem. B* **2014**, *2*, 5168.
[5] M. Moreno-Couranjou, R. Mauchauffe, C. Detrembleur, P. Choquet, *J. Mater. Chem. B* **2018**, *6*, 614.
[6] B. R. Coad, M. Jasieniak, S. S. Griesser, H. J. Griesser, *Surf. Coat. Technol.* **2013**, *233*, 169.
[7] N. R. Mohamad, N. H. Marzuki, N. A. Buang, F. Uuyop, R. A. Wahab, *Biotechnol. Biotechnol. Equip.* **2015**, *29*, 205.
[8] C. Mas-Moruno *Peptides and Proteins as Biomaterials for Tissue Regeneration and Repair, Chapter 3: Surface Functionalization of Biomaterials for Bone Tissue Regeneration and Repair.*, Bone Tissue Regeneration and Repair. (Eds: A Mário, M Barbosa, L Cristina, Martins), Elsevier Ltd., Woodhead Publisher, **2018**, https://doi.org/10.1016/C2015-0-01811-1
[9] I. Bilem, P. Chevallier, L. Plawinski, E. D. Sone, M. C. Durrieu, G. Laroche, A. C. S. Biomater, *Sci. Eng.* **2017**, *3*, 2514.
[10] L. Padiolleau, C. Chanseau, S. Durrieu, P. Chevallier, G. Laroche, M. C. Durrieu, *ACS Appl. Bio Mater.* **2018**, *1*, 1800.
[11] C. Mas-Moruno, R. Fraioli, F. Albericio, J. M. Manero, F. J. Gil, *ACS Appl. Mater. Interfaces* **2014**, *6*, 6525.
[12] H. Lee, S. M. Dellatore, W. M. Miller, P. B. Messersmith, *Science* **2007**, *318*, 426.
[13] T. S. Sileika, D. G. Barrett, R. Zhang, K. Hang, A. Lau, P. B. Messersmith, *Angew. Chem., Int. Ed.* **2013**, *52*, 10766.
[14] E. Faure, C. Falentin-daudré, T. S. Lanero, C. Vreuls, G. Zocchi, C. Van De Weerdt, J. Martial, C. Jérôme, A. Duwez, C. Detrembleur, *Adv. Funct. Mater.* **2012**, *22*, 5271.
[15] H. Lee, J. Rho, P. B. Messersmith, *Adv. Mater.* **2009**, *21*, 431.
[16] D. Duday, C. Vreuls, M. Moreno, G. Frache, N. D. Boscher, G. Zocchi, C. Archambeau, C. Van De Weerdt, J. Martial, P. Choquet, *Surf. Coat. Technol.* **2013**, *218*, 152.
[17] G. Camporeale, M. Moreno-Couranjou, N. D. Boscher, C. Bebrone, R. Mauchauffée, V. De Weerdt, H. Cauchie, P. Favia, P. Choquet, *Plasma Processes Polym.* **2015**, *12*, 1208.
[18] R. Mauchauffé, S. Bonot, M. Moreno-Couranjou, C. Detrembleur, N. D. Boscher, C. Van De Weerdt, A. Duwez, P. Choquet, *Adv. Mater. Interfaces* **2016**, *3*, 1500520.
[19] U. Czuba, R. Quintana, M. Bourguignon, M. Moreno-Couranjou, M. Alexandre, C. Detrembleur, P. Choquet, *Adv. Healthcare Mater.* **2018**, *11*, 1701059.
[20] U. Czuba, R. Quintana, P. Lassaux, R. Bombera, G. Ceccone, J. Bañuls-Ciscar, M. Moreno-Couranjou, C. Detrembleur, P. Choquet, *Colloids Surf. B* **2019**, *178*, 120.
[21] J. Buxadera Palomero, *PhD thesis*, Universitat Politècnica de Catalunya **2017**, http://hdl.handle.net/2117/111232
[22] J. Schäfer, K. Fricke, F. Mika, Z. Pokorná, L. Zajíčková, R. Foest, *Thin Solid Films* **2017**, *630*, 71.
[23] E. Faure, C. Falentin-daudré, C. Jérôme, J. Lyskawa, D. Fournier, P. Woisel, C. Detrembleur, *Prog. Polym. Sci.* **2013**, *38*, 236.
[24] N. Patil, C. Jérôme, C. Detrembleur, *Prog. Polym. Sci.* **2018**, *82*, 34.
[25] W. Weidman, *J. Am. Chem. Soc.* **1966**, *88*, 5820.
[26] B. M. Al Meslmani, G. F. Mahmoud, T. Leichtweiß, B. Strehlow, F. O. Sommer, M. D. Lohoff, U. Bakowsky, *Mater. Sci. Eng., C* **2016**, *58*, 78.
[27] G. Sauerbrey, *Zeitschrift für Phys.* **1959**, *155*, 206.
[28] G. Liu, G. Zhang, *J. Phys. Chem. B* **2005**, *109*, 743.
[29] A. Conte, G. G. Buonocore, M. Sinigaglia, L. C. Lopez, P. Favia, R. D. Agostino, M. A. Nobile, *J. Food Prot.* **2008**, *71*, 119.
[30] C. Detrembleur, C. Van de Weerdt, C. Vreuls, R. Mauchauffe, M. Moreno-Couranjou, D. Boscher, Nicolas, P. Choquet, Patent WO2016050419 (A2), Plasma Deposition Method for catechol/quinone functionalised layers, Patent WO2016050419 (A2), **2016**.
[31] M. Yu, J. Hwang, T. J. Deming, *J. Am. Chem. Soc.* **1999**, *121*, 5825.
[32] D. Beamson, G. Briggs, *High Resolution XPS of Organic Polymers: The Scienta ESCA 300 Database*, John Wiley & sons Ltd, Chichester **1992**.
[33] S. Rella, E. Mazzotta, A. Caroli, M. De Luca, C. Bucci, *Appl. Surf. Sci.* **2018**, *447*, 31.
[34] L. Le Guehennec, M. A. Lopez-Heredia, B. Enkel, P. Weiss, Y. Amouriq, P. Layrolle, *Acta Biomater.* **2008**, *4*, 535.
[35] R. Sammons *Chapter 3 Biological Responses to Hydroxyapatite*, Hydroxyapatite (HAp) for Biomedical Applications (Ed: M Mucalo), Elsevier Ltd, **2015**.
[36] Y. Wu, H. Ma, D. Gu, J. He, *RSC Adv.* **2015**, *5*, 64520.

How to cite this article: Czuba U, Moreno-Couranjou M, Collard D, et al. Controlled co-immobilization of biomolecules on quinone-bearing plasma polymer films for multifunctional biomaterial surfaces. *Plasma Process Polym*. 2020;17:e2000090. https://doi.org/10.1002/ppap.202000090